doi:10.1093/brain/awt024 Brain 2013: 136; 1035–1047 | 1035

BRAIN
A JOURNAL OF NEUROLOGY

Identification of endothelin 2 as an inflammatory factor that promotes central nervous system remyelination

Tracy J. Yuen,[1,2,3,*] Kory R. Johnson,[4] Veronique E. Miron,[1] Chao Zhao,[2] Jacqueline Quandt,[3,†] Marie C. Harrisingh,[1] Matthew Swire,[1] Anna Williams,[1] Henry F. McFarland,[3] Robin J. M. Franklin[2] and Charles ffrench-Constant[1]

1 MRC Centre for Regenerative Medicine and MS Society/University of Edinburgh Centre for Translational Research, University of Edinburgh, Edinburgh, UK
2 Wellcome Trust MRC Cambridge Stem Cell Institute and Department of Veterinary Medicine, University of Cambridge, Cambridge, UK
3 Neuroimmunology Branch, National Institutes of Health, Bethesda, MD, USA
4 Bioinformatics Section, Information Technology and Bioinformatics Program, National Institute of Neurological Disorders and Stroke, National Institutes of Health, Bethesda, MD, USA

*Present address: Departments of Paediatrics and Neurosurgery, Eli and Edythe Broad Institute for Stem Cell Research and Regeneration Medicine and Howard Hughes Medical Institute, University of California San Francisco, USA
†Present address: Department of Pathology and Laboratory Medicine, Brain Research Centre, University of British Columbia, Canada

Correspondence to: Prof. Charles ffrench-Constant,
MRC Centre for Regenerative Medicine and multiple sclerosis Society/University of Edinburgh Centre for Translational Research,
Centre for Inflammation Research,
The Queen's Medical Research Institute,
University of Edinburgh, Edinburgh EH16 4TJ, UK.
E-mail: cffc@ed.ac.uk

Correspondence may also be addressed to: Prof. Robin Franklin, Wellcome-Trust MRC Cambridge Stem Cell Institute and Department of Veterinary Medicine, University of Cambridge, Madingley Road, Cambridge CB3 0ES, UK E-mail: rjf1000@cam.ac.uk

The development of new regenerative therapies for multiple sclerosis is hindered by the lack of potential targets for enhancing remyelination. The study of naturally regenerative processes such as the innate immune response represents a powerful approach for target discovery to solve this problem. By 'mining' these processes using transcriptional profiling we can identify candidate factors that can then be tested individually in clinically-relevant models of demyelination and remyelination. Here, therefore, we have examined a previously described *in vivo* model of the innate immune response in which zymosan-induced macrophage activation in the retina promotes myelin sheath formation by oligodendrocytes generated from transplanted precursor cells. While this model is not itself clinically relevant, it does provide a logical starting point for this study as factors that promote myelination must be present. Microarray analysis of zymosan-treated retinae identified several cytokines (CXCL13, endothelin 2, CCL20 and CXCL2) to be significantly upregulated. When tested in a cerebellar slice culture model, CXCL13 and endothelin 2 promoted myelination and endothelin 2 also promoted remyelination. In studies to identify the receptor responsible for this regenerative effect of endothelin 2, analysis of both remyelination following experimental demyelination and of different stages of multiple sclerosis lesions in human post-mortem tissue revealed high levels of endothelin receptor type B in oligodendrocyte lineage cells. Confirming a role for this receptor in remyelination, small molecule agonists and antagonists of endothelin receptor type B administered in slice cultures promoted and inhibited remyelination, respectively. Antagonists of endothelin receptor type B also inhibited remyelination of experimentally-generated demyelination *in vivo*. Our work therefore

Received July 26, 2012. Revised December 11, 2012. Accepted December 21, 2012

identifies endothelin 2 and the endothelin receptor type B as a regenerative pathway and suggests that endothelin receptor type B agonists represent a promising therapeutic approach to promote myelin regeneration.

Keywords: remyelination; inflammation; oligodendrocytes; endothelin; regeneration; multiple sclerosis

Abbreviations: ET-1 = endothelin 1; ET-2 = endothelin 2; ET-A = endothelin receptor type A; ET-B = endothelin receptor type B

Introduction

The study of naturally occurring regenerative stimuli that promote remyelination provides a powerful strategy for discovering new targets to promote repair in multiple sclerosis. One such stimulus is the innate immune response. While CNS inflammation such as that seen in multiple sclerosis is usually thought to cause damage—a view supported by experimental models where the adaptive immune system is used to induce demyelination such as experimental autoimmune encephalomyelitis—the use of models in which the adaptive immune response is absent, such as toxin-induced demyelination, reveals a powerful regenerative role for the innate immune response (Kotter *et al*., 2001, 2005; Li *et al*., 2005; Chari *et al*., 2006; Glezer *et al*., 2006). As part of this response, a key role for macrophages is demonstrated by impaired remyelination following their depletion (Kotter *et al*., 2001). Two possible mechanisms by which macrophages enhance remyelination can be envisaged: the ability of macrophages to clear myelin debris, which is known to inhibit repair (Kotter *et al*., 2006; Ruckh *et al*., 2012) or secretion of regenerative factors such as cytokines. In support of the latter, we have shown that activation of the innate immune response by zymosan, a Toll-like receptor-2 ligand, increases the extent of myelination following transplantation of oligodendrocyte precursor cells into a CNS environment that lacks myelin—the nerve fibre layer of the retina (Setzu *et al*., 2006). Identification of these regenerative cytokines of the innate immune response therefore represents a logical next step in the search for therapeutic targets that enhance remyelination in multiple sclerosis.

While the experimental model of retinal inflammation and transplantation that we used above is clearly not a translational endpoint for studies to identify factors that enhance remyelination, it does provide an appropriate starting point for this next step. By performing a transcriptional analysis of the retinal innate immune response following zymosan injection (a response we know includes factors that enhance myelination by transplanted oligodendrocyte precursor cells) we can 'mine' this naturally regenerative process to assemble a list of candidate cytokines that can then be tested in other, progressively more complex models to identify those that do promote remyelination in areas of the CNS vulnerable to demyelination. We emphasize that the goal of such a study is target cytokine validation using clinically-relevant models of remyelination, not a detailed analysis of the (clinically-irrelevant) retinal myelination model that is used only to extract the initial list of candidate cytokines upregulated following induction of innate immunity. Using this strategy, we describe here the identification of endothelin 2 (ET-2, now known as *EDN2*) and the endothelin receptor type B (ET-B, now known as *EDNRB*) receptor as a novel therapeutic target and pathway for enhancing remyelination in multiple sclerosis.

Materials and methods

Retinal injection surgeries and analysis

All procedures were performed in compliance with UK Home Office regulations. Zymosan (12.5 μg/μl) or PBS was injected transvitreally into the retinae of adult female Fisher rats aged 9–14 weeks as previously described (Setzu *et al*., 2004, 2006). At various time points, retina samples were dissected out and cut in half. Half was fixed in 4% paraformaldehyde for histological analysis, and the other half preserved in RNAlater (Qiagen) for RNA extraction using a Qiagen RNeasy® Mini Kit.

Retina histology

Fixed retinae were blocked in 20% normal goat serum (Sigma) in 0.3% Triton PBS and then incubated overnight at 4°C with antibodies against CD68 (Serotec, 1:100) and GFAP (Dako, 1:100). Staining was visualized using appropriate secondary antibodies, and retinae were flat-mounted and examined using confocal microscopy.

Microarray and bioinformatics analysis

Microarray analysis was run on all samples using Illumina rat RefSeq chips containing 22 226 genes. To identify differentially-expressed genes, the statistical programming language R was used (http://cran.r-project/org/). Raw microarray data were log (base = 2) transformed and quantile normalized. The Tukey Box plot, covariance-based principal component analysis scatter plot, and correlation-based heat map were used to assure data quality. System noise was defined to equal the normalized expression value at which the locally weighted scatter plot smoothing fit of the observed coefficient of variation per gene by the observed mean expression per gene becomes non-linear. Genes not having at least one normalized expression value across all samples greater than system noise were discarded as 'non-informative'. Genes not discarded were subject to the two-factor ANOVA (treatment × time). Genes found to have a Benjamini Hochberg false discovery rate multiple comparison corrected P-value < 0.05 were deemed 'informative' and subject to the Tukey Honestly Significant Difference *post hoc* test to identify differentially-expressed genes (uncorrected P-value < 0.05) at 3 days, 7 days and 14 days post-injection.

Oligodendrocyte precursor cell assays

Oligodendrocyte precursor cell cultures were prepared from neonatal Sprague Dawley rats as described previously (McCarthy and de Vellis, 1980; Laursen *et al*., 2009). Cells were plated with tested factors (ET-2

from Sigma, remainder from R&D Systems). To assess proliferation, cells were stained 48 h later for bromodeoxyuridene (BrdU Labeling and Detection Kit I, Roche) and Hoechst (bisBenzamide, Sigma). To assess survival or differentiation, cells were plated in SATO medium with factors and 0.5% foetal calf serum and allowed to differentiate for 72 h. Apoptotic cells were visualized using the ApopTag® Apoptosis Detection Kit (Millipore). To examine differentiation, cells were stained 72 h following plating for myelin basic protein (AbD Serotec) and Hoechst. In all analyses, five ×20 field images from each well plated were taken using an Axioplan Fluorescence microscope (Carl Zeiss) with Openlab imaging software. Three separate cell isolations were used, with three separate chambers from each isolation plated for each factor and dose. To examine ERK signalling, cultures were grown on 35 mm plastic dishes for 2–3 days then starved for 4–5 h before stimulation with ET-2 (10 ng/ml, Sigma) or the ET-B selective agonist BQ3020 (100 ng/ml, Sigma). For the antagonist experiment, cells were pretreated with the ET-B selective antagonist BQ788 (100 ng/ml) for 15 min before stimulation with BQ3020 for 15 min. Following treatment, cells were harvested and lysates for western blot were prepared as previously described by Gadea *et al*. (2008). Antibodies were diluted in 4% bovine serum albumin (Sigma) in Tris-buffered saline with 0.1% Tween 20, phospho-p44/42 MAPK (Erk1/2) (1:2000) and p44/42 MAPK (Erk1/2) (1:1000) (both from Cell Signaling Technology).

Cerebellar slice cultures

Following decapitation, brains of post-natal Day 0–1 CD1 mice were dissected out into Eagle's medium with Earle's salts medium (MEM). Sagittal slices (350 μm) of the cerebellum and underlying hindbrain were cut using a McIlwain tissue chopper, and then placed on Millipore Millicell-CM™ organotypic culture inserts in medium containing MEM, Earle's balanced salt solution, heat-inactivated horse serum, GlutaMAX™, Fungizone®, and penicillin–streptomycin (each from Invitrogen), and glucose (Sigma). Factors were added at the desired concentrations, and fresh medium supplemented with factors every 2 days. Demyelination was induced after 14 days in culture without added factors by the addition of 0.5% lysolecithin (Sigma) to the medium for 20 h, after which slices were transferred back to either control medium or medium containing factors of interest, and maintained for an additional 14 days.

At 12 days *in vitro* for myelination and 28 days *in vitro* for remyelination, slices were fixed and stained. Confocal *z*-stacks were acquired (12 slices) with a Leica SPE confocal microscope and images analysed using NIH ImageJ. Only slices with intact cytoarchitecture were chosen for analysis, and imaging was focused on the areas of the cerebellum that contain parallel tracts of axons. Per cent area stained for Caspr or NFH was calculated and the degree of myelination or remyelination quantified by a ratio of per cent area stained for Caspr to per cent area stained for NFH. Using NIH ImageJ, Caspr images were carefully thresholded to only include areas of discrete, punctate paranodal Caspr staining, and to exclude more diffuse, internodal Caspr staining. Three separate slice isolations were used, with 8–12 slices analysed from each isolation for each factor and dose.

Cerebellar slice culture immunohistochemistry

Slices were fixed with 4% paraformaldehyde, blocked with 3% heat-inactivated horse serum, 2% bovine serum albumin, 0.25% Triton™ X-100, and then incubated in primary antibodies overnight at 4°C. Primary antibodies used were: anti-neurofilament 200 kDa (Encor Biotech, 1:4000), anti-myelin basic protein (AbD Serotec, 1:250), anti-Caspr (AbCam, 1:500), and anti-sodium channel (Sigma, 1:750). Staining was visualized by incubation in appropriate secondary antibodies at room temperature.

Electron microscopy

Cerebellar slice cultures were fixed overnight in 2.5% glutaraldehyde in 0.2 M sodium cacodylate and post-fixed in osmium tetroxide. The tissue was then dehydrated through ascending alcohols before embedding in resin. Cured resin blocks were trimmed and 1 μm sections cut, stained with toluidine blue and examined by light microscopy. Selected areas were further trimmed and ultrathin sections cut with a diamond blade onto copper grids using an ultramicrotome. Copper grid mounted ultrathin sections were stained with uranyl acetate and lead citrate and examined by transmission electron microscopy.

Focal demyelination

Demyelinating lesions were induced bilaterally by stereotactic injections of 4 μl of 0.01% ethidium bromide into the caudal cerebellar peduncles using a Hamilton syringe (Woodruff and Franklin, 1999). Female 3-month-old Sprague Dawley rats (180–210 g) were used for expression experiments and female 6-month-old rats (230–270 g) for delivery experiments. Non-radioactive *in situ* hybridization for ET-B in combination with immunostaining with antibodies against GFAP (Dako, 1:1000), CD68 (Serotec, 1:400), Olig2 (Millipore, 1:500) and Nkx2.2 (DHSB, 1:100) was then performed as described previously (Sim *et al*., 2002).

For delivery experiments, animals were administered 200 μl of a 23 nmol solution of BQ788, BQ3020, or saline by daily intraperitoneal injections from 7 days post-lesion to 14 days post-lesion (the time during which oligodendrocyte precursor cell differentiation is taking place). Animals were euthanized at 21 days post-lesion by perfusion with 4% glutaraldehyde under deep anaesthesia. The brain was dissected out, post-fixed and then cut into 1 mm transverse sections. Samples were embedded in resin, and 1 μm sections cut using a Leica RM2065 microtome and collected on glass slides. Following staining with 1% toluidine blue, sections from all three experimental conditions were ranked by an observer blind to these conditions for their level of remyelination as judged by light microscopy.

Multiple sclerosis lesion analysis

Brain tissue was obtained through a UK prospective donor scheme with full ethical approval from the UK Multiple Sclerosis Tissue Bank (MREC/02/2/39). Multiple sclerosis diagnosis was confirmed by Dr F. Roncaroli (Imperial College London) and clinical history was provided by Dr R. Nicholas (Imperial College London). Snap-frozen tissue was sectioned at 10 μm and classified according to the International Classification of Neurological Disease using Luxol fast blue staining and Oil Red O. We analysed five control blocks, six acute active lesions, four chronic active lesions, 14 chronic inactive lesions and 19 remyelinated lesions. Sections were fixed in 4% paraformaldehyde for 1 h, and permeabilized in methanol for 10 min at −20°C. Following antigen retrieval and blocking endogenous peroxidase activity (EnVision™ blocking solution, Dako), rabbit anti-endothelin B receptor primary antibody (1:200, Abcam) was applied overnight in a humid chamber at 4°C. Anti-mouse peroxidase conjugated secondary antibody was applied for 2 h at room temperature and stains visualized by 3,3′diaminobenzidene chromagen and

light microscopy (Olympus BX61); sections were counterstained with Hoechst. For co-localization stains, sections were blocked with 10% normal horse serum and 0.1% Triton^{TM} X-100 for 1 h, antibodies applied overnight as before, and fluorescently conjugated secondary antibodies applied for 2 h with Hoechst counterstain. Fluorescent images were acquired by confocal microscopy (Leica SPE). Immunopositive cells were counted per lesion and counts were multiplied accordingly to determine density of immunopositive cells/mm^2 and statistical comparisons were done using Mann–Whitney test where $P < 0.05$ was considered to be statistically significant.

Results

CXCL13, endothelin 2, CCL20 and CXCL2 are upregulated in an inflammatory environment supporting myelination

Our first goal was to assemble a list of candidate factors within the innate immune response that could be used for further studies on clinically relevant models to identify those that represent promising targets for enhancing regeneration. Thus, we used our previously described model of zymosan injection into the retina (Setzu *et al.*, 2006). We performed a microarray analysis of gene expression at four time points (0, 3, 7 and 14 days post-injection) using the same zymosan injection protocol as in our previous work and using PBS injected retina at each time point as controls and Illumina Rat RefSeq chips for hybridization. An inbred rat strain (Fisher) was used to reduce variations due to genetic background, and three rats were used to provide three biological replicates at each time point and condition. Histological analysis (Fig. 1) confirmed changes in the retina consistent with an activation of the innate immune system. An increase in CD68-positive macrophages/activated microglia was seen with the greatest effect at 3 days post-injection. Increased GFAP expression, indicating a reactive response in retinal astrocytes (Müller cells), was also seen at all post-injection time points and was greatest at 14 days post-injection. Following microarray data normalization, we first excluded genes with an expression level below the noise level (15 086 of 22 226 genes), defined as the point at which the relationship between mean values and the coefficient of variation becomes non-linear. Then we used a two-factor ANOVA with a false discovery rate set at 5% to identify significant differences in gene responses. This analysis identified 44 upregulated genes at 3 days, eight upregulated genes at 7 days and 69 upregulated genes at 14 days (Supplementary Table 1). Within these differentially expressed genes, however, only four growth factors or cytokines were present: CXCL13, ET-2, CCL20 and CXCL2 (Supplementary Table 1). At 3 days, CCL20 was found to be upregulated 7.4-fold, CXCL2 4.8-fold, and ET-2 2.5-fold. None of these four genes were found to be significantly upregulated at 7 days. At 14 days, however, CXCL13 was found to be upregulated 16.1-fold, CCL20 13.4-fold, CXCL2 8.6-fold and ET-2 2.4-fold. The upregulation of CXCL13 and ET-2 following zymosan injection was validated using quantitative real-time PCR (Supplementary Fig. 1).

CXCL13 and endothelin 2 promote myelination

Next, we determined which of these candidate cytokines might provide potential targets for remyelination therapies by narrowing the list to include only those that enhanced myelination by endogenous oligodendrocyte precursor cells in normally-myelinated regions of the CNS. To do so, we used the simplest available assay in which oligodendrocyte precursor cells generate myelin-forming oligodendrocytes in intact CNS tissue—cerebellar slice cultures. Explant cultures from newborn mice were prepared by cutting sagittal sections of cerebellum and examined at 12 days *in vitro* (Fig. 2A). At this point myelination is not yet fully complete, allowing us to observe a potential acceleration by added factors.

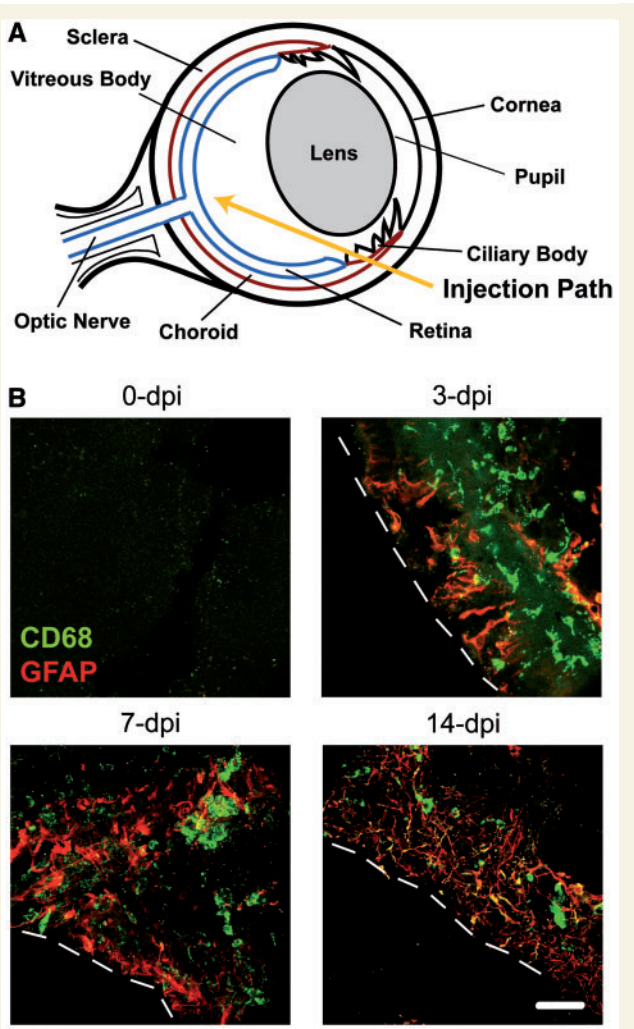

Figure 1 An inflammatory response is seen following injection of zymosan. (**A**) Diagram of transvitreal retinal injection into the rat eye. (**B**) Sections of retinae at time points used for microarray analysis stained for macrophages/activated microglia (CD68, green) and astrocytes (GFAP, red). Note the predominance of macrophages/microglia at 3 days post-injection (dpi) and astrocytes at 14 days post-injection. The dotted line denotes the edge of the retina. Scale bar = 30 μm.

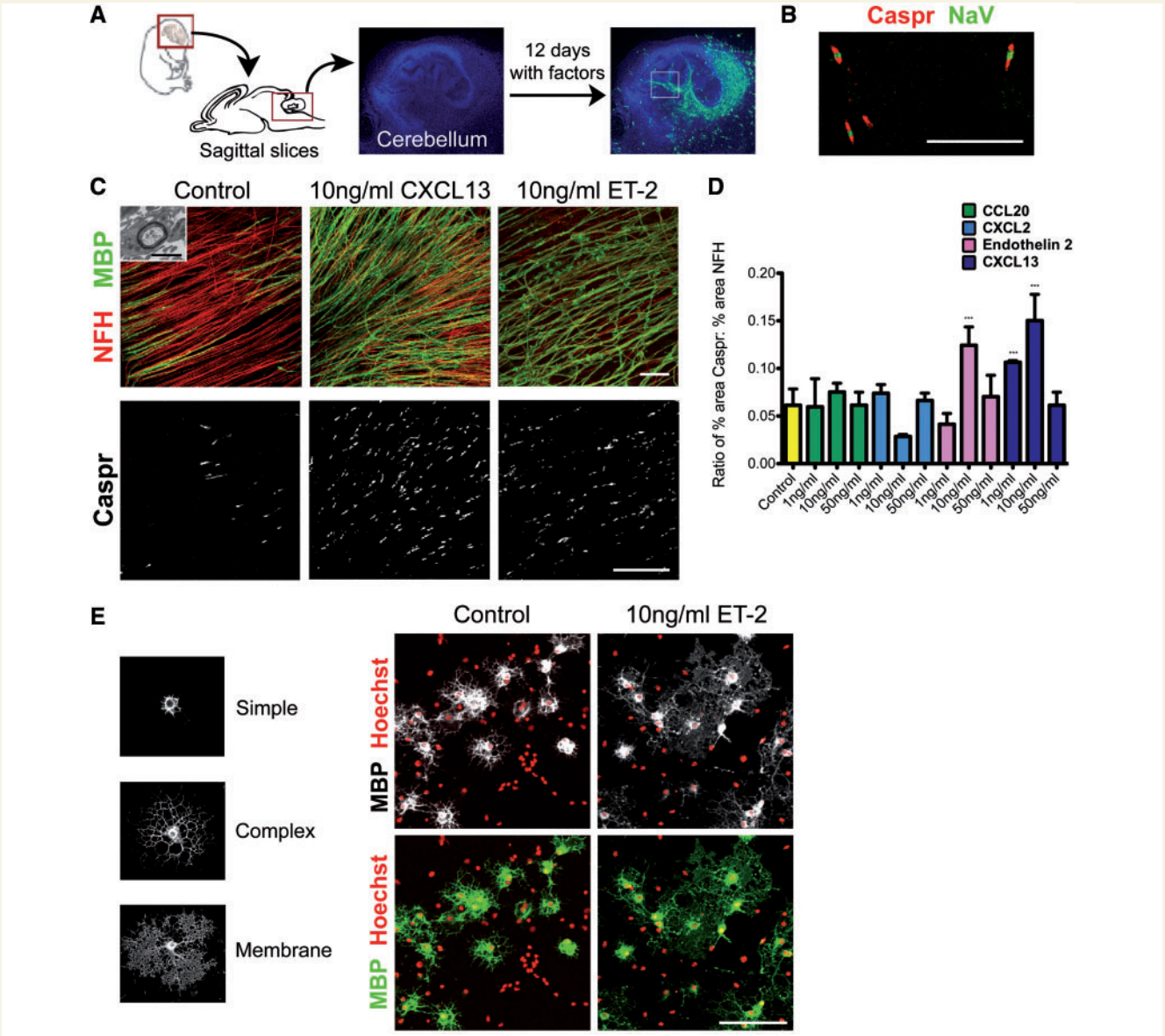

Figure 2 ET-2 and CXCL13 promote myelination in cerebellar slice cultures. (**A**) Experimental schematic for myelinating slice cultures. Following 12 days in culture, parallel tracts of myelin (MBP, green; Hoescht, blue) are seen in the cerebellum. (**B**) Confirmation of myelination in the slices, as shown by formation of nodes of Ranvier revealed by characteristic concentrations of Caspr (red) and voltage-dependent sodium channels (NaV, green) at the paranodes and nodal axolemma. (**C**) Confocal *z*-stacks of slice cultures labelled to show axons (NFH, red), myelin (MBP, green), and paranodes (Caspr, white) demonstrate an increase in myelination with CXCL13 or ET-2 (ET-2) as revealed by an increase in number of paranodes and MBP+ internodes. *Top left inset:* An electron micrograph of a myelinated axon in the slices, confirming the formation of compacted myelin. (**D**) Quantification of myelination in slice cultures. Ratios of the area stained for Caspr to the area stained for NFH (measuring paranode formation) are shown. Values shown are mean + SD ($n = 3$). The data are analysed by one-way ANOVA with Dunnett's multiple comparison test, and significant differences (***$P < 0.001$) are shown. (**E**) ET-2 promotes shape changes associated with myelination. For clarity, the same oligodendrocytes are shown in two ways: as green on black and also as white on black images, with nuclei in red. Note the increased process complexity and MBP+ myelin sheet formation by oligodendrocytes in culture as they proceed from 'simple' to 'complex' and finally to 'membrane' morphology. Scale bars: **B** = 20 μm; **C** inset = 2 μm; **C** = 30 μm; **E** = 100 μm.

To quantify changes of myelination in response to added factors, we took advantage of the finding that the generation of compact myelin is associated with a change in the expression pattern of the axonal adhesion molecule Caspr, with exclusion from the internodal areas and its localization at the paranodal regions of the nodes of Ranvier (Eisenbach *et al.*, 2009). This change in expression pattern was revealed in our slice cultures by immunofluorescent studies showing a concentration of voltage-dependant Na+ channels at the nodal axolemma and Caspr at the paranode (Fig. 2B), with electron microscopy directly confirming the presence of

compact myelin at this time (Fig. 2C inset). As in our recent study examining the effects of a Wnt pathway inhibitor (Fancy *et al*., 2011), we used image analysis to quantify myelination in the slices by calculating the area of Caspr immunostaining corresponding to paranodes, using a thresholding technique to exclude the diffuse and weaker internodal Caspr immunostaining, and expressed this as a ratio of the area of axons. This unbiased approach allows accurate quantification of paranodal Caspr even in the presence of the variability of axon orientation and density observed in these cultures. This showed that CXCL13 and ET-2 promoted myelination significantly at 10 ng/ml, with CXCL13 also having a weak effect at 1 ng/ml (Fig. 2C and D). Neither factor was effective at the highest concentration (Fig. 2D). No effect was seen at any concentration of CCL20 or CXCL2 (Fig. 2D).

To determine whether this enhanced myelination represented an effect of CXCL13 and ET-2 that would increase the overall number of oligodendrocytes, we examined purified cultures of dissociated oligodendrocyte precursor cells and oligodendrocytes grown in the absence of axons and the presence of each of the four factors. We did not observe changes in proliferation, survival or differentiation [as measured by the expression of myelin basic protein (MBP)], each of which would be expected to increase oligodendrocyte numbers. Thus, quantification of proliferation by bromodeoxyuridene uptake showed that, apart from a very small reduction in proliferation seen at 1 ng/ml of CXCL13, none of the four factors altered oligodendrocyte precursor cell proliferation (Supplementary Fig. 2). Equally, we observed no changes in apoptosis in the cultures (Supplementary Fig. 3). Finally, there was no increase in the number of MBP+ cells generated within the cultures by CXCL13 or ET-2, although small effects were seen with the two factors that had no effect on myelination in the slices, CXCL2 and CCL20 (Supplementary Fig. 4).

Next, therefore, we tested an alternative explanation for enhanced myelination in the slices—an increased level of myelin formation by individual oligodendrocytes. We reasoned that myelin formation by an individual MBP+ oligodendrocyte could be measured by the formation of complex cellular processes and by the elaboration of membranous sheets of myelin. Thus, as in our recent study examining the effect of RXRγ signalling on oligodendrocyte differentiation (Huang *et al*., 2011), we performed a quantitative analysis of myelin sheet formation by scoring individual oligodendrocytes as having 'simple' (short, non-interdigitating processes), 'complex' (longer, interdigitating processes, but not membrane sheets), or 'membrane' morphology (processes containing MBP+ membrane sheets) (Fig. 2E). If a factor promotes myelin sheet formation, the number of cells with a simple morphology would decrease and the number of complex and membrane-forming cells would increase. Such changes were seen with ET-2 (at both 10 and 50 ng/ml) (Fig. 2E) and CXCL13 (at 10 ng/ml). The ratio of the most differentiated, membrane morphology cells increased from 0.107 ± 0.084 (mean $\pm$ SD) for controls to 0.480 ± 0.072 (ET-2, 10 ng/ml, $P < 0.001$), 0.232 ± 0.061 (ET-2, 50 ng/ml, $P < 0.001$), and 0.354 ± 0.088 (CXCL13, 10 ng/ml, $P < 0.001$). In contrast, there was no effect on oligodendrocyte morphology with the addition of CCL20 or CXCL2, showing that the stimulation of complex processes and myelin sheets in culture was a property only of CXCL13 and ET-2. We conclude from these experiments on cultured cells that the enhanced myelination seen in the slices reflects increased myelin formation by individual oligodendrocytes rather than any effect on proliferation, survival and differentiation.

Endothelin 2 enhances remyelination in explant cultures

Having narrowed the list of cytokines identified from the transcriptional profiling of the innate immune response to two factors that enhance myelination, we next examined whether these factors could also promote remyelination. To do this we modified the slice culture protocol above to allow myelination to take place for 14 days, after which there are extensive numbers of MBP+ internodes. Lysolecithin was then added for 20 h to demyelinate the slices, and then cultured for an additional 14 days during which remyelination occurs (Fig. 3A) (Miron *et al*., 2010; Huang *et al*., 2011; Zhang *et al*., 2011). Demyelination and remyelination (Fig. 3A and B) were visualized and quantified by using image analysis to measure the area of paranodal Caspr as above and as in our recent studies on Axin 2 (Fancy *et al*., 2011). In contrast with the experiments examining myelination in these slices, the addition of CXCL13 had no effect on remyelination (Fig. 3C and D). ET-2, however, enhanced remyelination at 10 ng/ml while 50 ng/ml had no effect (Fig. 3C and D). As in earlier studies of myelination, the formation of nodes of Ranvier and compact myelin in the cerebellar slices (here by remyelination) was confirmed with immunofluorescent and electron microscopy studies showing both demyelination following lysolecithin exposure and subsequent remyelination (Fig. 3E and F).

Endothelin receptor type B is required for remyelination

Having now narrowed the list of candidate cytokines to a single factor that promotes remyelination, ET-2, we next considered the question of which receptor is likely to be responsible. ET-2 is recognized by two G-protein coupled receptors termed endothelin receptors type A and B (ET-A and ET-B, respectively). In rodent cells of the oligodendrocyte lineage ET-B is more highly expressed than ET-A, as measured by immunofluorescence, western blotting and real-time-PCR of isolated cells (Gadea *et al*., 2009). ET-B is also highly expressed on human foetal oligodendrocyte precursor cells isolated by cell sorting and then subjected to transcriptional profiling (Sim *et al*., 2011). These isolated oligodendrocyte precursor cells are specifically those that were shown to have a high myelinogenic potential. ET-B signalling also makes a greater contribution than ET-A to endothelin receptor-induced phosphorylation of ERK (Gadea *et al*., 2009), the significance of which is highlighted by recent work showing that ERK2 is essential for timely myelination (Fyffe-Maricich *et al*., 2011). Together these suggest that ET-B signalling is likely to be responsible for the effects of ET-2 on oligodendrocytes that we observed above. To confirm this, we analysed the effects of a well-characterized ET-B-specific small molecule agonist (BQ3020) and antagonist

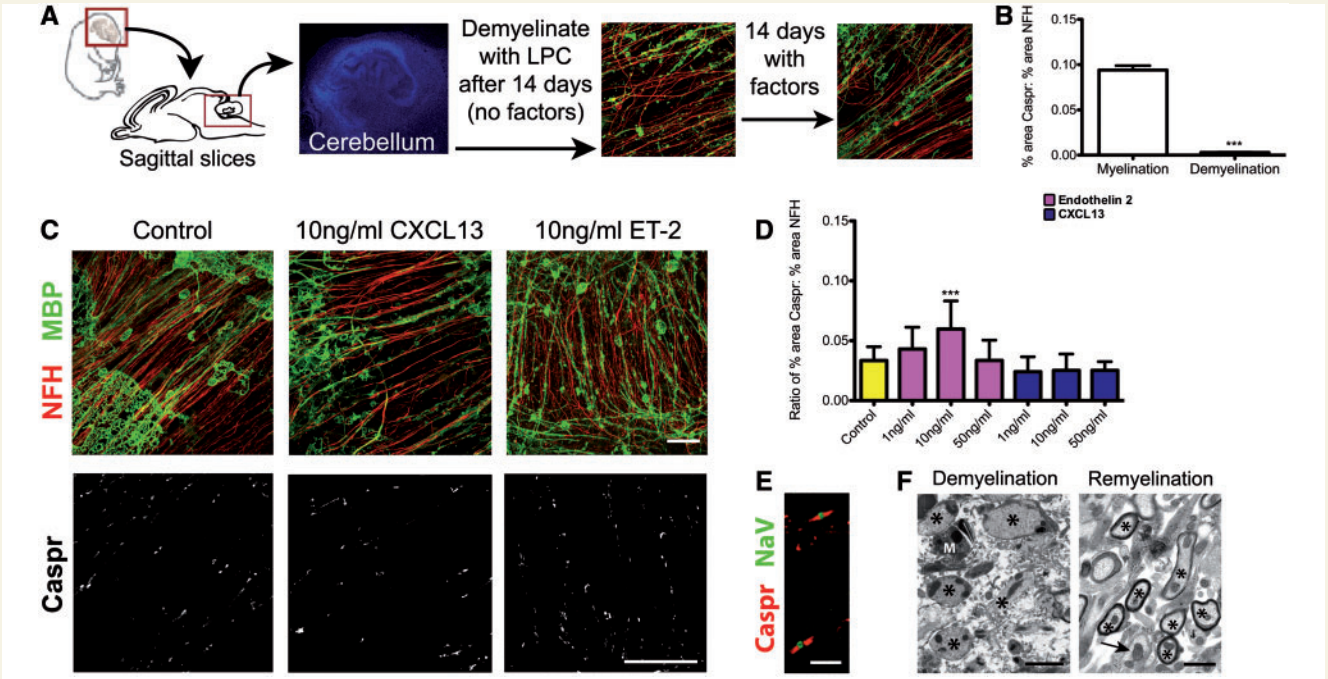

Figure 3 ET-2 but not CXCL13 promotes remyelination in cerebellar slice cultures. (**A**) Experimental schematic for remyelinating slice cultures. Following exposure to lysolecithin (LPC), fully myelinated cultures are demyelinated without damage to axons. After removal of lysolecithin, cultures are maintained for 14 additional days and remyelinate (MBP, green; NFH, red). (**B**) Quantification demonstrates a loss of myelin after exposure to lysolecithin. Control slices not exposed to lysolecithin (myelination) are compared with those exposed to lysolecithin (demyelination) at 15 days *in vitro*. The data are analysed by *t*-test and the significant difference (***$P < 0.001$) is shown. (**C**) Confocal *z*-stacks of cerebellar slice cultures (labelled and analysed as in Fig. 2) demonstrate an increase in remyelination following the addition of ET-2. (**D**) Quantification demonstrates an increase in remyelination with 10 ng/ml ET-2. Values shown are mean + SD ($n = 3$). The data are analysed by one-way ANOVA with Dunnett's multiple comparison test, and the significant difference (***$P < 0.001$) is shown. (**E**) Confirmation of remyelination in the slices as revealed by formation of nodes of Ranvier, labelled as in Fig. 2, and by (**F**) electron microscopy showing the loss of myelin following lysolecithin (*left*) and the presence of compact myelin following remyelination (*right*). In the demyelination panel, asterisks denote demyelinated axons. Note the high neurofilament density. M = reactive microglial cell. In the remyelination panel, asterisks denote remyelinated axons, and the arrow denotes a demyelinated axon surrounded by oligodendrocyte processes, likely in the process of being remyelinated. Scale bars: **C** = 30 μm; **E** = 10 μm; **F** = 2 μm.

(BQ788) (Ihara *et al*., 1992; Ishikawa *et al*., 1994) on ERK phosphorylation and on cell behaviour in the cell culture assays. As shown previously for endothelin 1 (ET-1) (Gadea *et al*., 2009) oligodendrocyte precursors treated with ET-2 showed rapid ERK phosphorylation (Supplementary Fig. 5). A similar effect was seen with the ET-B agonist BQ3020, and this could be blocked by the BQ788 antagonist (Supplementary Fig. 5). In the oligodendrocyte morphology assay, we found that the selective ET-B antagonist BQ788 inhibited myelin sheet formation at all concentrations tested (1–100 ng/ml), as revealed by a reduction in the number of cells with a differentiated, complex morphology and a corresponding increase in the fraction of those with a simple morphology from 0.212 ± 0.047 (control, mean ± SD) to 0.351 ± 0.028 (1 ng/ml, $P < 0.001$), 0.470 ± 0.041 (10 ng/ml, $P < 0.001$), 0.444 ± 0.033 (50 ng/ml, $P < 0.001$), and 0.433 ± 0.058 (100 ng/ml, $P < 0.001$) (Fig. 4A). In contrast, the selective ETB agonist BQ3020 increased the fraction of cells forming myelin sheets from 0.202 ± 0.042 (control, mean ± SD) to 0.335 ± 0.034 (50 ng/ml, $P < 0.001$) and 0.350 ± 0.032 (100 ng/ml, $P < 0.001$) (Fig. 4A). Activation of ET-B signalling therefore appears to mimic the effect of ET-2 on both ERK phosphorylation and on myelin formation, while the effect of the antagonist suggests that ET-B signalling in response to endogenous ligands contributes to the regulation of oligodendrocyte morphology during myelin formation.

Next, therefore, we determined whether ET-B was also expressed during remyelination in rodent models and, importantly for a study designed to identify potential targets for remyelination therapies, in human multiple sclerosis lesions. For the rodent studies we used a well-characterized model of remyelination, a focal lesion model in which demyelination is induced in the rat caudal cerebellar peduncle by injection of ethidium bromide (Fig. 4B) (Woodruff and Franklin, 1999; Sim *et al*., 2002). This *in vivo* model is advantageous for our study as there is no ongoing damage after the initial effects of the toxin and the tempo of the subsequent remyelination process is well defined; oligodendrocyte precursor cells repopulate the lesion at 5 days post-lesion, differentiate and initiate remyelination between 10–14 days post-lesion, and complete remyelination by 21–28 days post-lesion (Sim *et al*., 2002). First, we re-analysed our previously described microarray data set comparing gene expression profiles at 5, 14 and 28 days post-injection in the caudal cerebellar peduncle

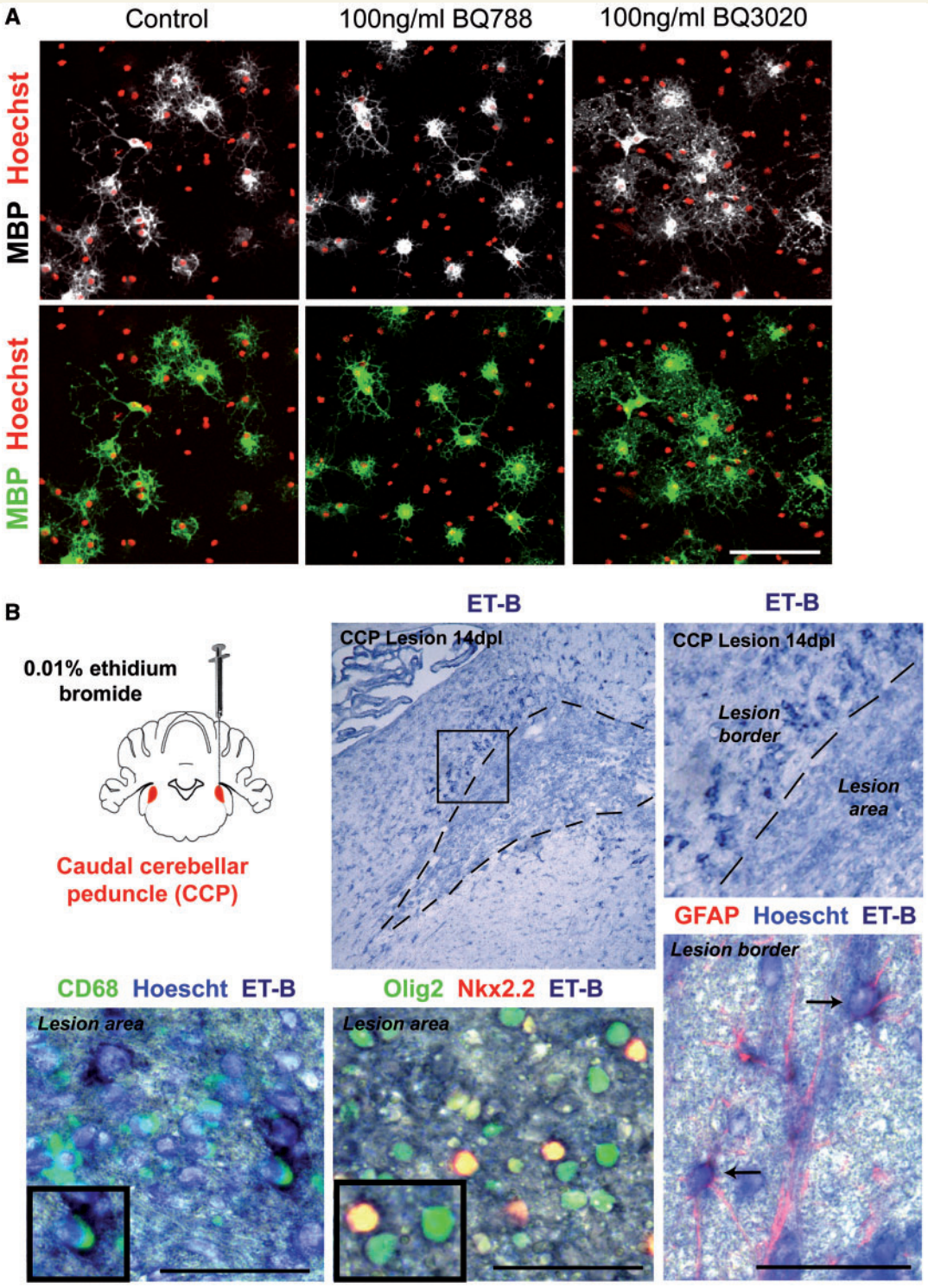

Figure 4 ET-B signalling affects myelin production by oligodendrocytes and ET-B receptors are expressed during remyelination. (**A**) Shape changes associated with myelination by oligodendrocytes are impeded by an ET-B antagonist (BQ788) and enhanced by an ET-B agonist (BQ3020), as shown by changes in process complexity and the formation of MBP+ myelin sheets. As in Fig. 2, the same oligodendrocytes are shown as both green on black and white on black images for clarity. (**B**) Experimental schematic of experimentally-induced focal lesions in the CCP of rats where *in situ* hybridization shows expression of ET-B at 14 days post-lesion (dpl). *Top left:* A low power view of the lesion (with lesion border denoted by a dotted line). Note increased *in situ* hybridization reaction product in cells within the lesion, and also that ET-B is expressed in cells surrounding the lesion (box on low power image, shown in higher power on the *right*). *Bottom:* A higher power view from within the lesion or from the border (as labelled), combining *in situ* hybridization with immunostaining for CD68 (*left*) to identify macrophages/microglia, Olig2 and Nkx2.2 (*middle*) to identify oligodendrocyte lineage cells and GFAP (*right*) to identify astrocytes. Note that ET-B is expressed on macrophages/microglia and oligodendroglial cells within the lesion and on astrocytes at the lesion edge (arrows). Scale bars = 50 μm.

lesion. This showed a significant upregulation of ET-B between 5 and 14 days post-lesion (logFC 1.96, $P = 0.01$) corresponding to ~4-fold increase. We confirmed that this increase represented expression on oligodendroglial cells by *in situ* hybridization studies of these lesions at 14 days post-lesion. These experiments showed that ET-B was expressed within lesions (Fig. 4B), and combined *in situ* hybridization and immunohistochemistry experiments showed that expression was present on Olig2+ oligodendroglial cells and Nkx2.2+/Olig2+ oligodendrocyte precursor cells, with macrophages/microglia also expressing the receptor (Fig. 4B). ET-B was also strongly expressed on cells around the lesion border where co-labelling with an antibody against GFAP indicated that many of these cells were astrocytes (Fig. 4B).

To establish the connection between our data in experimental animals and clinical disease in humans we examined four categories of multiple sclerosis lesion by immunohistochemistry: acute active, chronic active, chronic inactive and remyelinated, with both the rim and centre of the chronic active lesions examined separately (Fig. 5A). Increased numbers of ET-B expressing

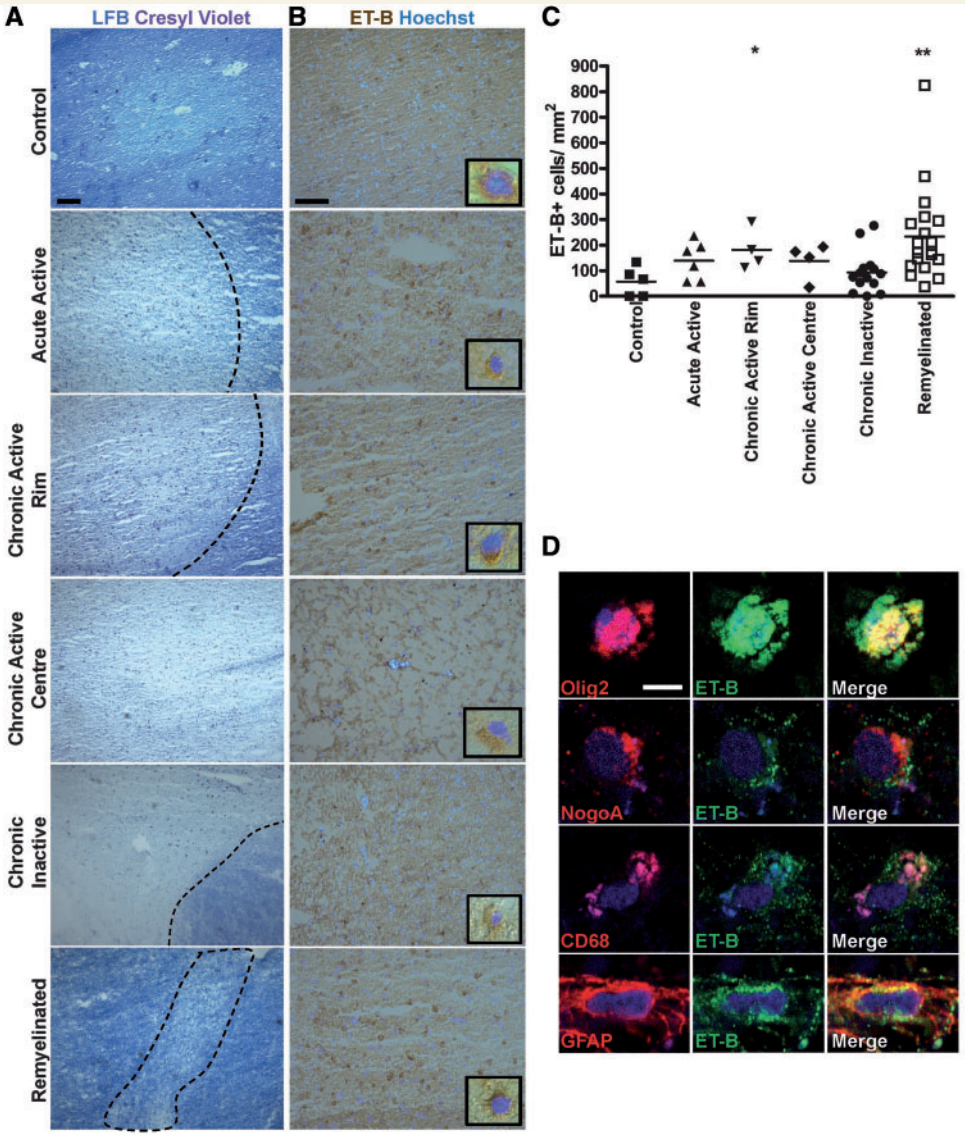

Figure 5 ET-B expression in multiple sclerosis lesions. Brain sections from a control and a multiple sclerosis patient. (**A**) Representative images of brain sections from control and multiple sclerosis patients stained for myelin by Luxol fast blue (LFB) and counterstained with haematoxylin. Lesion types include acute active, chronic active rim and centre, chronic inactive, and remyelinated, and are delineated by loss of myelin (dotted line). (**B**) Representative images of same lesions immunostained against endothelin B receptor and counterstained with Hoechst. (**C**) Densities of ET-B-positive cells per mm^2 in control tissue and multiple sclerosis lesions. Mann Whitney test, $*P < 0.05$, $**P < 0.01$. (**D**) ET-B is expressed in cells of the oligodendrocyte lineage (Olig2), mature oligodendrocytes (NogoA), microglia/macrophages (CD68), and astrocytes (GFAP). Nuclei marked with Hoechst (blue). Note that strong staining with DAB weakens Hoechst signal. Scale bars: A = 200 μm; B = 100 μm; D = 5 μm.

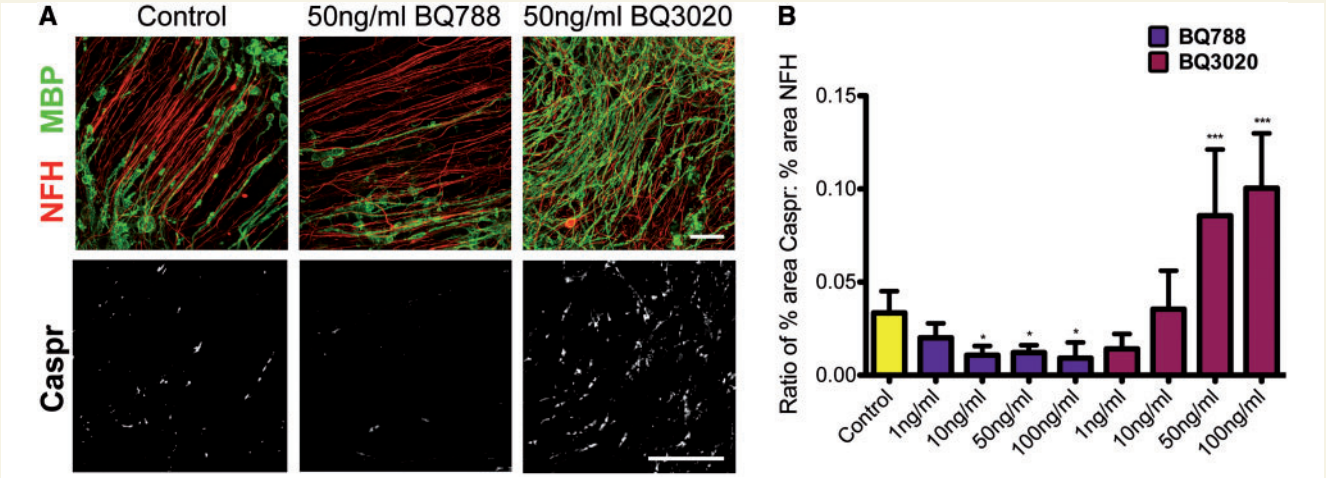

Figure 6 Modulating ET-B signalling using small-molecule compounds affects remyelination in *ex vivo* cerebellar explant cultures. (**A**) Confocal *z*-stacks of cerebellar slice cultures, labelled as in Fig. 2, demonstrate that ET-B signalling plays a role in remyelination. Scale bar = 30 μm. (**B**) Quantification as in Fig. 2 demonstrates a decrease in remyelination with the ET-B antagonist (BQ788) and an increase in remyelination with the ET-B agonist (BQ3020). Values shown are mean + SD ($n = 3$). The data are analysed by one-way ANOVA with Dunnett's multiple comparison test, and significant differences (***$P < 0.001$, *$P < 0.05$) are shown.

cells were seen in lesions (Fig. 5B), with this increase reaching significance for the rim of chronic active lesions and in remyelinated lesions (Fig. 5C)—both of which would be expected to contain oligodendrocyte precursor cells as they are areas of present or past regenerative activity. We confirmed directly that ET-B was expressed on oligodendrocyte precursor cells and differentiated oligodendrocytes in these lesions by demonstrating cells double labelled with Olig2 and NogoA, respectively (Fig. 5D). As in the experimental lesions, expression was also seen in macrophages/microglia and astrocytes, revealed by double labelling with CD68 and GFAP (Fig. 5D).

Having confirmed that both small molecule agonists or antagonists of ET-B promote or inhibit oligodendrocyte morphology changes that accompany myelination, and that ET-B is expressed on oligodendroglial cells during remyelination in rat and human, we asked whether agonists or antagonists of ET-B affected remyelination. In the *ex vivo* demyelinated cerebellar slice cultures analysed as above we found that blocking ET-B signalling with BQ788 at 10–100 ng/ml inhibited remyelination to levels below that seen in control slices, while activation of ET-B signalling with BQ3020 at 50–100 ng/ml enhanced remyelination (Fig. 6A and B). Interestingly, the level of remyelination seen with BQ3020 was greater than the maximal level observed with ET-2 (Fig. 3) suggesting that other ET-B ligands, such as ET-1, might also be able to contribute to remyelination through ET-B. Finally, we examined whether manipulating ET-B signalling could block or enhance CNS remyelination *in vivo*. Given the prior evidence from studies of horseradish peroxidase extravasation that the blood–brain barrier is defective in focal toxin lesions during remyelination (Felts and Smith, 1996), we used an intraperitoneal rather than an intracerebral route to administer the small molecule agonist and antagonist into the CNS. Following focal demyelination using the protocol described above, we injected saline, the ET-B agonist or ET-B antagonist intraperitoneally each day at 7–14 days post-lesion—the time of oligodendrocyte differentiation and initiation of remyelination. Animals were euthanized at 21 days post-lesion and semi-thin resin sections and ultrastructural analyses used to assess remyelination. We found that blocking ET-B signalling with the antagonist significantly impaired remyelination (Fig. 7A and B), although no effect of the agonist was observed in this model.

Discussion

Here we show that ET-2 is a cytokine upregulated following activation of the innate immune response that enhances myelination and remyelination by oligodendrocytes. The ET-B mediates these regenerative effects. This receptor is expressed on oligodendrocyte precursor cells during remyelination in experimental rodent models and also on oligodendrocyte precursor cells within multiple sclerosis lesions, and agonists and antagonists of the receptor promote or inhibit myelination and remyelination in explant cultures. Moreover, ET-B activity is necessary for remyelination *in vivo*, as antagonists inhibit the normal regenerative response following toxin-induced demyelination in the adult rat. Together these results support the logic of our strategy of profiling the innate immune response to identify new targets for remyelination therapies, and identify endothelin signalling as a regenerative pathway in the CNS that leads to remyelination.

ET-2 belongs to the endothelin family of three 21 amino acid peptides: ET-1, -2 and -3 (Yanagisawa *et al.*, 1988; Kawanabe and Nauli, 2011). ET-1 is widely expressed and implicated in a number of pathological processes including vasoconstriction, inflammation and tumour metastasis (Said *et al.*, 2011). It is also expressed in the spinal cord of animals with experimental autoimmune encephalomyelitis, produced mainly by CD68-positive macrophages and activated microglia (Shin *et al.*, 2001). ET-2

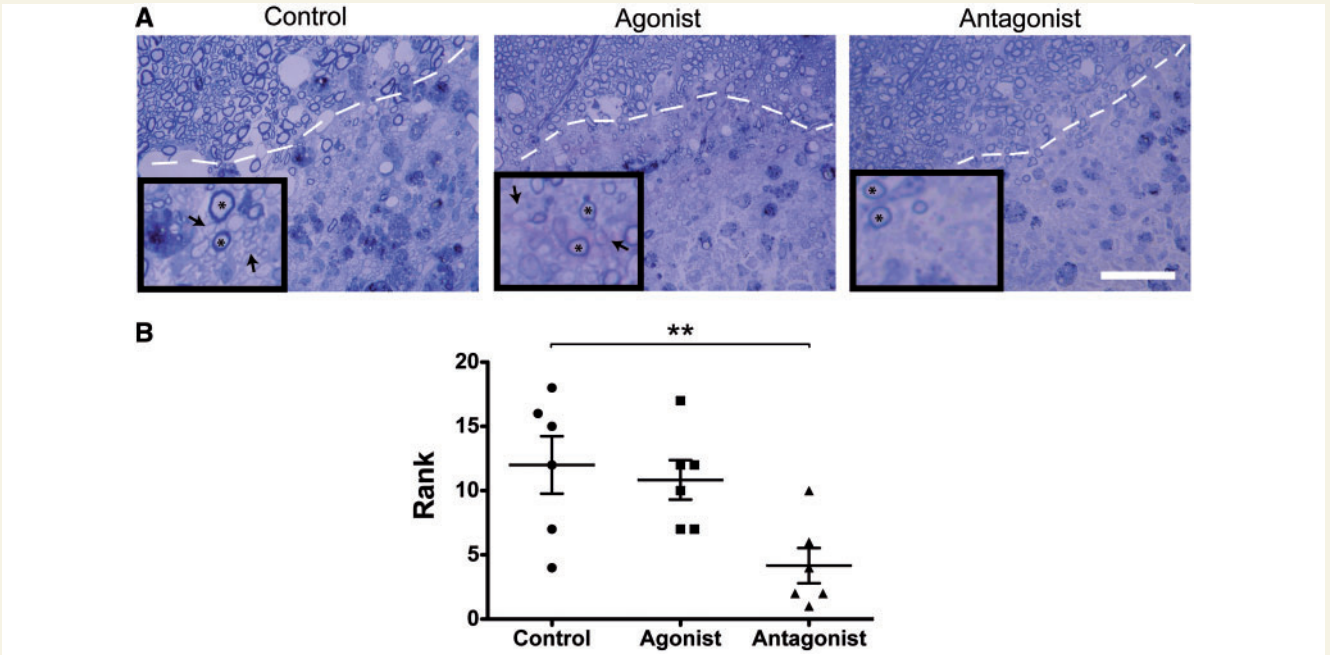

Figure 7 Administration of an ET-B antagonist inhibits remyelination *in vivo* following demyelinating lesion in the CCP. (**A**) Toluidine blue staining of semi-thin resin sections of saline-injected controls animals, ET-B agonist-treated animals, and ET-B antagonist-treated animals. Normally myelinated axons outside the lesion are shown in the *top left* corner of each picture, and dotted lines denote the lesion border. Within the lesion, remyelinated axons (arrows) and unaffected myelinated axons (asterisks) can be seen. Scale bar = 50 μm. (**B**) Ranking analysis of the degree of remyelination in all three experimental groups shows decreased remyelination in ET-B antagonist-treated ($n = 6$) animals compared with saline-treated control rats ($n = 6$). Highest rank = highest degree of CNS remyelination. The data were analysed by Kruskal-Wallis one-way ANOVA with Dunn's multiple comparison test and the significant difference (**$P < 0.01$) is shown.

(the form we have identified in this study) is much less widely expressed and has not previously been reported either in the CNS or in association with inflammation, in contrast with ET-1 and -3, which are produced by both astrocytes and macrophages (Ehrenreich *et al*., 1990; MacCumber *et al*., 1990; Gadea *et al*., 2009). All these endothelins will bind to two endothelin receptors—ET-A and ET-B (Arai *et al*., 1990; Sakurai *et al*., 1990; Davenport, 2002). Both are G protein coupled receptors, but their association with different sets of G proteins results in their activation of separate downstream signalling pathways, for example, ET-A promotes vasoconstriction whereas ET-B can promote vasodilation (Aramori and Nakanishi, 1992; Rosano *et al*., 2009; Kawanabe and Nauli, 2011). Within the CNS, a role in pain sensation is well described (Khodorova *et al*., 2009), and here again the two receptors may have differing functions as the expression pattern of ET-A and ET-B in sensory nerves is distinct, being on small diameter axons and satellite glial cells, respectively (Pomonis *et al*., 2001).

Previous studies of endothelin signalling have suggested a possible indirect effect on regeneration, as ET-B is highly expressed on astrocytes around the border of the demyelinated lesion, as shown in this study, and both ET-1 (Gadea *et al*., 2008) and ET-B signalling (Koyama *et al*., 1999; Rogers *et al*., 2003) promote astrogliosis. These activated astrocytes may therefore release extracellular matrix and/or soluble factors that promote remyelination. Evidence for a direct effect of endothelin signalling on oligodendrocyte lineage cells came first from a developmental study showing that ET-1 secreted by astrocytes promotes oligodendrocyte precursor cell migration and inhibits the acquisition of differentiation markers such as MBP (Gadea *et al*., 2009). Experiments with receptor agonists and antagonists revealed a more significant role for ET-B than ET-A in migration (Gadea *et al*., 2009). Our study now shows that ET-B also has a role in remyelination, and increases myelin formation by cultured oligodendrocytes. In contrast, neither ET-1 (Gadea *et al*., 2009) or ET-2 appear to have a role in the regulation of proliferation or survival of oligodendroglial cells during remyelination. Together these studies highlight the potential importance of endothelin signalling and ET-B in an example of CNS regeneration—remyelination—by directly enhancing at least two of the steps required: the recruitment of precursors and the elaboration of myelin by differentiated cells. This conclusion as to the role of endothelin signalling is further supported by our experiment showing that inhibition of ET-B by a peripherally-administered small molecule antagonist impairs remyelination of focal lesions *in vivo*. The lack of any effect of the ET-B agonists *in vivo* remains to be explained and may reflect inappropriate dosing and/or an effect of ET-B signalling on other tissues such as blood vessels that prevent a regenerative response; however, it should be noted that remyelination in young adult rodents as used here is already extremely efficient and it may therefore be difficult to reveal any beneficial effect.

One discrepancy between our study using ET-2 and the previous work above using ET-1 is the effect on oligodendrocyte differentiation. We found no effect of ET-2 on the number of MBP+ cells while Gadea *et al*. (2009) found an inhibition of MBP expression with ET-1. Given that both endothelins bind to the same receptors, this was unexpected. One possible mechanism could be the presence of distinct co-receptors associating with each endothelin receptor that bind to one or the other endothelin. Another possibility is the triggering of distinct downstream pathways dependent on the level of ligand binding and receptor activation. An example of this is provided by another growth factor receptor, PDGFRα, where high and low levels of signalling result in the activation of PI3K (needed for oligodendrocyte precursor cell proliferation and migration) or PLCγ signalling (only needed for oligodendrocyte precursor cell migration), respectively (McKinnon *et al*., 2005). However, the observation from another study of ET-1 showing increased MBP in cultured oligodendrocytes (Jung *et al*., 2011) in apparent contradiction to the results of Gadea *et al*. (2009), suggests additional complexity that further experiments are required to unravel.

Our finding that ET-2 and ET-B signalling promote the changes in shape that lead to myelin membrane formation, but have no effect on the number of cells expressing myelin proteins such as MBP, is interesting in that it highlights the distinct regulation of two components of oligodendrocyte biology that are often considered as a single process—differentiation and myelin formation. From a cell biology perspective, however, linking regulation of shape and gene expression is not necessarily appropriate given the very different molecular mechanisms involved, and our work adds to other observations that emphasize this (Rosenberg *et al*., 2008). So, for example, myelination in rat optic nerve begins at the retinal end of the nerve whereas myelin protein expression is first seen in oligodendrocytes at the chiasmal end (Colello *et al*., 1995). Experiments in co-culture of neurons and oligodendrocytes show that NGF inhibits myelination by already differentiated MBP+ oligodendrocytes (Chan *et al*., 2004), and a similar result is seen with PDGF and FGF2 (Wang *et al*., 2007). Together with experiments showing that the extracellular matrix substrate merosin promotes myelin sheet formation by cells cultured without axons without any effect on the number of MBP+ cells (Buttery and ffrench-Constant, 1999), these results clearly show that the pathways controlling shape and gene expression can be regulated directly and independently in oligodendrocytes.

As well as identifying a novel signalling pathway that promotes remyelination, our present findings add significantly to our understanding of how inflammation might promote regeneration. Earlier studies of the CNS have identified regenerative properties of inflammation by the description of macrophage-derived oncomodulin as a factor that promotes retinal ganglion axon regeneration (Yin *et al*., 2006, 2009) and by the finding that mice lacking inflammatory cytokines IL1β or TNFα have delayed remyelination following demyelination caused by the administration of cuprizone (Arnett *et al*., 2001; Mason *et al*., 2001). Taken together with these studies, our results emphasize how the inflammatory response represents a rich source of potential novel regenerative factors for therapeutic exploration.

Acknowledgements

The authors would like to thank Andrew Jarjour, Lisbeth Laursen, David Coutts, and Anna Setzu for technical assistance.

Funding

This work was supported by the United Kingdom Multiple Sclerosis Society (to C.ff.C., R.J.M.F.); National Multiple Sclerosis Society (to C.ff.C., R.J.M.F.); and the Wellcome Trust (to C.ff.C.) T.J.Y. was supported by the National Institutes of Health-University of Cambridge Graduate Partnerships Program and the International Biomedical Research Alliance.

Supplementary material

Supplementary material is available at *Brain* online.

References

Arai H, Hori S, Aramori I, Ohkubo H, Nakanishi S. Cloning and expression of a cDNA encoding an endothelin receptor. Nature 1990; 348: 730–2.

Aramori I, Nakanishi S. Coupling of two endothelin receptor subtypes to differing signal transduction in transfected Chinese hamster ovary cells. J Biol Chem 1992; 267: 12468–74.

Arnett HA, Mason J, Marino M, Suzuki K, Matsushima GK, Ting JP. TNF alpha promotes proliferation of oligodendrocyte progenitors and remyelination. Nat Neurosci 2001; 4: 1116–22.

Buttery PC, ffrench-Constant C. Laminin-2/integrin interactions enhance myelin membrane formation by oligodendrocytes. Mol Cell Neurosci 1999; 14: 199–212.

Chan JR, Watkins TA, Cosgaya JM, Zhang C, Chen L, Reichardt LF, et al. NGF controls axonal receptivity to myelination by Schwann cells or oligodendrocytes. Neuron 2004; 43: 183–91.

Chari DM, Zhao C, Kotter MR, Blakemore WF, Franklin RJM. Corticosteroids delay remyelination of experimental demyelination in the rodent central nervous system. J Neurosci Res 2006; 83: 594–605.

Colello RJ, Devey LR, Imperato E, Pott U. The chronology of oligodendrocyte differentiation in the rat optic nerve: evidence for a signaling step initiating myelination in the CNS. J Neurosci 1995; 15: 7665–72.

Davenport AP. International Union of Pharmacology. XXIX. Update on endothelin receptor nomenclature. Pharmacol Rev 2002; 54: 219–26.

Ehrenreich H, Anderson RW, Fox CH, Rieckmann P, Hoffman GS, Travis WD, et al. Endothelins, peptides with potent vasoactive properties, are produced by human macrophages. J Exp Med 1990; 172: 1741–8.

Eisenbach M, Kartvelishvily E, Eshed-Eisenbach Y, Watkins T, Sorensen A, Thomson C, et al. Differential clustering of Caspr by oligodendrocytes and Schwann cells. J Neurosci Res 2009; 87: 3492–501.

Fancy SP, Harrington EP, Yuen TJ, Silbereis JC, Zhao C, Baranzini SE, et al. Axin2 as regulatory and therapeutic target in newborn brain injury and remyelination. Nat Neurosci 2011; 14: 1009–16.

Felts PA, Smith KJ. Blood-brain barrier permeability in astrocyte-free regions of the central nervous system remyelinated by Schwann cells. Neuroscience 1996; 75: 643–55.

Fyffe-Maricich SL, Karlo JC, Landreth GE, Miller RH. The ERK2 mitogen-activated protein kinase regulates the timing of oligodendrocyte differentiation. J Neurosci 2011; 31: 843–50.

Gadea A, Aguirre A, Haydar TF, Gallo V. Endothelin-1 regulates oligodendrocyte development. J Neurosci 2009; 29: 10047–62.

Gadea A, Schinelli S, Gallo V. Endothelin-1 regulates astrocyte proliferation and reactive gliosis via a JNK/c-Jun signaling pathway. J Neurosci 2008; 28: 2394–408.

Glezer I, Lapointe A, Rivest S. Innate immunity triggers oligodendrocyte progenitor reactivity and confines damages to brain injuries. FASEB J 2006; 20: 750–2.

Huang JK, Jarjour AA, Nait Oumesmar B, Kerninon C, Williams A, Krezel W, et al. Retinoid X receptor gamma signaling accelerates CNS remyelination. Nat Neurosci 2011; 14: 45–53.

Ihara M, Saeki T, Fukuroda T, Kimura S, Ozaki S, Patel AC, et al. A novel radioligand [125I]BQ-3020 selective for endothelin (ETB) receptors. Life Sci 1992; 51: PL47–52.

Ishikawa K, Ihara M, Noguchi K, Mase T, Mino N, Saeki T, et al. Biochemical and pharmacological profile of a potent and selective endothelin B-receptor antagonist, BQ-788. Proc Natl Acad Sci USA 1994; 91: 4892–6.

Jung KJ, Kim DW, Lee HN, Lee YS, Lee SJ, Che JH, et al. The role of endothelin receptor A during myelination of developing oligodendrocytes. J Korean Med Sci 2011; 26: 92–9.

Kawanabe Y, Nauli SM. Endothelin. Cell Mol Life Sci 2011; 68: 195–203.

Khodorova A, Richter J, Vasko MR, Strichartz G. Early and late contributions of glutamate and CGRP to mechanical sensitization by endothelin-1. J Pain 2009; 10: 740–9.

Kotter MR, Li WW, Zhao C, Franklin RJM. Myelin impairs CNS remyelination by inhibiting oligodendrocyte precursor cell differentiation. J Neurosci 2006; 26: 328–32.

Kotter MR, Setzu A, Sim FJ, Van Rooijen N, Franklin RJM. Macrophage depletion impairs oligodendrocyte remyelination following lysolecithin-induced demyelination. Glia 2001; 35: 204–12.

Kotter MR, Zhao C, van Rooijen N, Franklin RJM. Macrophage-depletion induced impairment of experimental CNS remyelination is associated with a reduced oligodendrocyte progenitor cell response and altered growth factor expression. Neurobiol Dis 2005; 18: 166–75.

Koyama Y, Takemura M, Fujiki K, Ishikawa N, Shigenaga Y, Baba A. BQ788, an endothelin ET(B) receptor antagonist, attenuates stab wound injury-induced reactive astrocytes in rat brain. Glia 1999; 26: 268–71.

Laursen LS, Chan CW, ffrench-Constant C. An integrin-contactin complex regulates CNS myelination by differential Fyn phosphorylation. J Neurosci 2009; 29: 9174–85.

Li WW, Setzu A, Zhao C, Franklin RJM. Minocycline-mediated inhibition of microglia activation impairs oligodendrocyte progenitor cell responses and remyelination in a non-immune model of demyelination. J Neuroimmunol 2005; 158: 58–66.

MacCumber MW, Ross CA, Snyder SH. Endothelin in brain: receptors, mitogenesis, and biosynthesis in glial cells. Proc Natl Acad Sci USA 1990; 87: 2359–63.

Mason JL, Suzuki K, Chaplin DD, Matsushima GK. Interleukin-1beta promotes repair of the CNS. J Neurosci 2001; 21: 7046–52.

McCarthy KD, de Vellis J. Preparation of separate astroglial and oligodendroglial cell cultures from rat cerebral tissue. J Cell Biol 1980; 85: 890–902.

McKinnon RD, Waldron S, Kiel ME. PDGF alpha-receptor signal strength controls an RTK rheostat that integrates phosphoinositol 3′-kinase and phospholipase Cgamma pathways during oligodendrocyte maturation. J Neurosci 2005; 25: 3499–508.

Miron VE, Ludwin SK, Darlington PJ, Jarjour AA, Soliven B, Kennedy TE, et al. Fingolimod (FTY720) enhances remyelination following demyelination of organotypic cerebellar slices. Am J Pathol 2010; 176: 2682–94.

Pomonis JD, Rogers SD, Peters CM, Ghilardi JR, Mantyh PW. Expression and localization of endothelin receptors: implications for the involvement of peripheral glia in nociception. J Neurosci 2001; 21: 999–1006.

Rogers SD, Peters CM, Pomonis JD, Hagiwara H, Ghilardi JR, Mantyh PW. Endothelin B receptors are expressed by astrocytes and regulate astrocyte hypertrophy in the normal and injured CNS. Glia 2003; 41: 180–90.

Rosano L, Cianfrocca R, Masi S, Spinella F, Di Castro V, Biroccio A, et al. Beta-arrestin links endothelin A receptor to beta-catenin signaling to induce ovarian cancer cell invasion and metastasis. Proc Natl Acad Sci USA 2009; 106: 2806–11.

Rosenberg SS, Kelland EE, Tokar E, De la Torre AR, Chan JR. The geometric and spatial constraints of the microenvironment induce oligodendrocyte differentiation. Proc Natl Acad Sci USA 2008; 105: 14662–7.

Ruckh JM, Zhao JW, Shadrach JL, van Wijngaarden P, Rao TN, Wagers AJ, et al. Rejuvenation and regeneration in the aging central nervous system. Cell Stem Cell 2012; 10: 96–103.

Said N, Smith S, Sanchez-Carbayo M, Theodorescu D. Tumor endothelin-1 enhances metastatic colonization of the lung in mouse xenograft models of bladder cancer. J Clin Invest 2011; 121: 132–47.

Sakurai T, Yanagisawa M, Takuwa Y, Miyazaki H, Kimura S, Goto K, et al. Cloning of a cDNA encoding a non-isopeptide-selective subtype of the endothelin receptor. Nature 1990; 348: 732–5.

Setzu A, ffrench-Constant C, Franklin RJM. CNS axons retain their competence for myelination throughout life. Glia 2004; 45: 307–11.

Setzu A, Lathia JD, Zhao C, Wells K, Rao MS, ffrench-Constant C, et al. Inflammation stimulates myelination by transplanted oligodendrocyte precursor cells. Glia 2006; 54: 297–303.

Shin T, Kang B, Tanuma N, Matsumoto Y, Wie M, Ahn M, et al. Intrathecal administration of endothelin-1 receptor antagonist ameliorates autoimmune encephalomyelitis in Lewis rats. Neuroreport 2001; 12: 1465–8.

Sim FJ, McClain CR, Schanz SJ, Protack TL, Windrem MS, Goldman SA. CD140a identifies a population of highly myelinogenic, migration-competent and efficiently engrafting human oligodendrocyte progenitor cells. Nat Biotechnol 2011; 29: 934–41.

Sim FJ, Zhao C, Penderis J, Franklin RJM. The age-related decrease in CNS remyelination efficiency is attributable to an impairment of both oligodendrocyte progenitor recruitment and differentiation. J Neurosci 2002; 22: 2451–9.

Wang Z, Colognato H, ffrench-Constant C. Contrasting effects of mitogenic growth factors on myelination in neuron-oligodendrocyte co-cultures. Glia 2007; 55: 537–45.

Woodruff RH, Franklin RJM. Demyelination and remyelination of the caudal cerebellar peduncle of adult rats following stereotaxic injections of lysolecithin, ethidium bromide, and complement/anti-galactocerebroside: a comparative study. Glia 1999; 25: 216–28.

Yanagisawa M, Kurihara H, Kimura S, Tomobe Y, Kobayashi M, Mitsui Y, et al. A novel potent vasoconstrictor peptide produced by vascular endothelial cells. Nature 1988; 332: 411–5.

Yin Y, Cui Q, Gilbert HY, Yang Y, Yang Z, Berlinicke C, et al. Oncomodulin links inflammation to optic nerve regeneration. Proc Natl Acad Sci USA 2009; 106: 19587–92.

Yin Y, Henzl MT, Lorber B, Nakazawa T, Thomas TT, Jiang F, et al. Oncomodulin is a macrophage-derived signal for axon regeneration in retinal ganglion cells. Nat Neurosci 2006; 9: 843–52.

Zhang H, Jarjour AA, Boyd A, Williams A. Central nervous system remyelination in culture–a tool for multiple sclerosis research. Exp Neurol 2011; 230: 138–48.